Comptes Rendus

Chimie

Elise Bouderlique, Ellie Tang, Joëlle Perez, Hang-Korng Ea, Felix Renaudin, Amélie Coudert, Sophie Vandermeersch, Dominique Bazin, Jean-Philippe Haymann, Camille Saint-Jacques, Vincent Frochot, Michel Daudon and Emmanuel Letavernier

Inflammation plays a critical role in 2,8-dihydroxyadenine nephropathy

Microcrystalline pathologies: Clinical issues and nanochemistry / *Pathologies microcristallines : questions cliniques et nanochimie*

Inflammation plays a critical role in 2,8-dihydroxyadenine nephropathy

Elise Bouderlique [a, b]**, Ellie Tang** [a, b]**, Joëlle Perez** [a, b]**, Hang-Korng Ea** [c, d, e]**,
Felix Renaudin** [c, d, e]**, Amélie Coudert** [c, e]**, Sophie Vandermeersch** [a, b]**,
Dominique Bazin** [f]**, Jean-Philippe Haymann** [a, b, g]**, Camille Saint-Jacques** [a, b, g]**,
Vincent Frochot** [a, b, g]**, Michel Daudon** [a, b, g] **and Emmanuel Letavernier** [*, a, b, g]

[a] Sorbonne Universités, UPMC Univ Paris 06, UMR S 1155, F-75020, Paris, France

[b] INSERM, UMR S 1155, F-75020, Paris, France

[c] Université de Paris, département de médecine générale, 75018 Paris, France

[d] Hôpital Lariboisière, service de rhumatologie, pôle locomoteur, AP-HP, 2, rue Ambroise Paré 75010 Paris, France

[e] INSERM U1132 Bioscar, Paris 75010, France

[f] Laboratoire de Chimie Physique, CNRS UMR 8000, Université Paris XI, 91405 Orsay, France

[g] Physiology Unit, AP-HP, Hôpital Tenon, F-75020, Paris, France

Current address: Service des Explorations Fonctionnelles Multidisciplinaires, Hôpital TENON, 4 rue de la Chine, 75020 Paris, France (E. Letavernier)

E-mails: elise.bouderlique@inserm.fr, ellieyali.tang@hotmail.com, perezjoelle@yahoo.fr, hang-korng.ea@aphp.fr, Felix.renaudin@gmail.com, amelie.coudert@inserm.fr, sophie.vandermeersch@upmc.fr, dominique.bazin@u-psud.fr, jean-philippe.haymann@aphp.fr, camille.saint-jacques@aphp.fr, vincent.frochot@aphp.fr, michel.daudon@aphp.fr, emmanuel.letavernier@aphp.fr

Abstract. Adenine phosphoribosyltransferase (APRT) deficiency is a genetic disease characterized by an increased production of 2,8 dihydroxyadenine (2,8-DHA) precipitating in urine, leading to a crystalline nephropathy and end-stage renal disease. Here, we describe the high prevalence of granuloma (88%) in biopsies from patients with APRT deficiency. A murine model of 2,8-DHA nephropathy was generated, showing that anakinra or dexamethasone, combined with allopurinol, improved renal function to a larger extent than allopurinol alone, the standard therapy. Inflammation plays a critical role in the development of 2,8-DHA nephropathy, and therapy based upon drugs targeting innate immunity could improve renal function recovery.

Keywords. 2,8-Dihydroxyadenine, Adenine phosphoribosyl transferase (APRT), Kidney, Inflammation, Interleukin-1 beta.

Published online: 9 August 2021

---

[*] Corresponding author.

1. Introduction

Adenine phosphoribosyltransferase (APRT) deficiency is an autosomal recessive genetic disease [1–4]. This purine metabolism disorder results in an increased production and urinary excretion of 2,8 dihydroxyadenine (2,8-DHA) which is poorly soluble in urine, leading to recurrent urolithiasis and crystalline nephropathy. Actually, the main feature of this disease is the development of a chronic kidney disease resulting from crystallites precipitation in renal tubule, engulfment of crystallites by tubular epithelial cells and interstitial accumulation of 2,8-DHA and, finally, renal fibrosis. In the absence of a specific treatment, patients develop end-stage renal disease (ESRD). As renal transplantation does not cure the enzymatic deficiency, kidney transplant recipients are also affected by a high rate of recurrence leading to graft loss if the disease has not been diagnosed previously [5–7].

The disease is considered to be very rare and a majority of the cases have been reported in Iceland, France and Japan [4,8–11]. A missense (homozygous) mutation in exon 3 (Asp65Val) accounts for all cases of APRT deficiency in Iceland, suggesting the existence of a founder effect [4,12]. In Japan, a missense mutation in exon 5 (Met136MThr) affects 70% of patients [11]. By contrast, in 53 cases of APRT deficiency (from 43 families) identified at a single institution in France, 18 distinct mutations have been identified [9]. As suggested by Edvardsson *et al.* APRT could be massively unrecognized [4]. Actually, the estimated pathogenic mutation frequency in various populations could range from 0.4 to 1.2% [3,4, 10]. This suggests that homozygous or compound heterozygous carriers should be at least 1:50,000–100,000, i.e. 3000 cases in the USA and 9000 cases in Europe for instance. On the other hand, a recent study based upon six population genomic databases reported that the large number of cases in Japan and Iceland was consistent with a founder effect in these populations. In other countries, the minor allele frequency of pathogenic variants seems relatively low, suggesting that there is no widespread underdiagnosis of this nephropathy [13]. In France, many cases have been diagnosed with the help of crystalluria, morphoconstitutional kidney stone analysis including Fourier transform infrared (FTIR) spectroscopy and FTIR microscopy evidencing the crystalline phase in kidney biopsies, including kidney graft biopsies [9,14–16]. Measurement of enzyme activity in red blood cell lysates and genetic analyses were usually performed after identification of crystals and one may hypothesize that many patients with undiagnosed chronic kidney disease are affected by APRT deficiency. The widespread use of whole-exome sequencing in patients with unidentified nephropathy and who are candidates for an allograft should be informative in a near future.

There is a need for an early diagnosis as there is an efficient treatment: xanthine oxidoreductase inhibitors, allopurinol and febuxostat, which decrease 2,8-DHA synthesis and excretion in urine [17]. If initiated early, a lifelong therapy associated with high fluid intake may stabilize kidney function. Nevertheless, renal function recovery is often limited and there may be a place for other therapeutics to improve renal function recovery [7,18].

Klinkhammer *et al.* highlighted recently the important role of innate immunity in 2,8-DHA crystalline nephropathy, and described the presence of granuloma in a murine model of the disease [19]. As we have observed frequent and massive macrophage infiltrates and granuloma-like structures in biopsies from patients affected by APRT, we assessed systematically inflammatory infiltrates in a series of 17 biopsies. We performed *in vivo* animal studies to highlight the role of inflammation in this disease. In addition, we hypothesized that targeting the immune response induced by 2,8-DHA crystalline deposits might be protective and showed that corticosteroids or anakinra may improve renal outcome, when added to the conventional therapy (allopurinol), in a model of 2,8-DHA nephropathy.

2. Material and methods

2.1. *Human kidney tissue biopsies*

Seventeen biopsies from 17 patients affected by APRT deficiency were analyzed, including 12 biopsies performed in kidney grafts. All biopsies were sent to Tenon and Necker hospitals, Paris, to diagnose the nature of the crystalline nephropathy. Kidney tissues were fixed in formalin and embedded in paraffin. Four micrometer tissue sections were deposited on low emission microscope slides (MirrIR, Keveley Technologies, Tienta Sciences, Indianapolis, IN, USA). FTIR hyperspectral images

were recorded with a Spectrum spotlight 400 FTIR imaging system (Perkin Elmer Waltham, MA, USA), with a spatial resolution of 6.25 μm and a spectral resolution of 4 cm^{-1}. The spectra were recorded in the 4000–700 cm^{-1} mid-Infrared range. Each spectral image, covering a substantial part of the tissue, consisted of about 30,000 spectra. Histopathological lesions were analyzed in 4 μm sections stained with Masson Trichrome and Hematoxylin/Eosin staining, by two independent nephrologists trained in renal pathology. 2,8-DHA was identified using μ Fourier Transform InfraRed spectrometry in the 17 biopsies. For immunohistochemistry experiments, kidneys sections were dewaxed, heated in citric acid solution and next incubated with one of the following primary antibodies overnight at 4 °C: Anti-CD3 (Polyclonal, A0452 (Dako, Agilent, Santa Clara, CA, USA), Rabbit anti-mouse CD3 (Polyclonal, ab5690, Abcam, Cambridge, MA, USA), Rat anti-mouse pan-macrophages (Oxford Biotech, Oxford, UK), Anti-CD68 (PG-M1, M0876, Dako, Agilent, Santa Clara, CA, USA), Anti-CD163 (ab182422, Abcam, Cambridge, MA, USA). After washing, immunostaining was revealed with Histofine secondary antibodies (Nichirei Biosciences, Tokyo, Japan) and then revealed with AEC (k34769, Dako, Santa Clara, USA). Nuclei were counterstained with hematoxylin. Negative controls were performed by omitting the primary antibody. Tissue sections deposited on Mirr IR slides were examined with a Zeiss SUPRA55-VP Field Emission scanning Electron Microscope (Zeiss France, Marly-le-Roi, France). Measurements were performed at a low voltage (1.4 keV).

2.2. *Crystal synthesis*

2,8-DHA crystals were obtained from kidney stones containing 100% 2,8-DHA according to FTIR analysis. Stone fragments were ground in a mortar with 100% pure ethanol. Crystals were filtered in 100 μm sieve before washing in ethanol and warm sterilization. Monosodium urate (MSU) crystals were prepared with 500 mL of boiling water and 2 g of uric acid (U2625, Sigma Aldrich, St Louis, MO, USA). pH solution was maintained at 8 by adding NaOH (1 M). Solution was cooled and kept 24 h during crystals formation. Crystals were filtered in 100 μm sieve before washing in ethanol and warm sterilization and characterized by FTIR analysis. Monoclinic

calcium pyrophosphate dihydrate (mCPPD) crystals were synthesized and characterized as previously reported [20]. mCPPD crystals were characterized by X-ray diffraction (Seifert XRD-3000TT diffractometer with Cu Kα radiation, in the 2θ range 2°–70° with step size 0.02° and scan step time 16 s at 298 K), FTIR spectroscopy (Thermo Nicolet 5700 Fourier-transform infrared spectrometer) and scanning electron microscopy (SEM, Leo 435 VP microscope). All crystals were dispersed by brief sonication and suspended at 2 mg/mL in phosphate buffered saline (PBS). They were prepared under endotoxin-free conditions and tested negative with Pierce Limulus amebocyte Assay (Thermo Fisher Scientific, Waltham, MA, USA).

2.3. *Animal models*

Eight-week old male C57Bl/6J mice were used for *in vivo* experiments. After purchase, mice were housed one week before experimentation. All mice were housed and bred in similar conditions at INSERM UMR S 1155 Mouse Facility, with a 12-h dark/light cycle. All mice received standard chow (or adenine-enriched diet). All animal procedures were performed in accordance with the European Union and National Institutes of Health guidelines for the care and use of laboratory animals (Comité d'Ethique en Experimentation Charles Darwin C2EA-05). The project was authorized by the Health Ministry and local Ethics Committee (authorization numbers #13902 and #16615).

2.3.1. *Mouse air-pouch model*

Eight-week old male C57Bl/6J mice were used to perform an air-pouch model (six animals/group). Air pouches were created by two dorsal subcutaneous injections of 3 mL of sterile air (day 0 and day 3), under isoflurane anesthesia. At day 6, PBS (1 mL) in control mice or crystals (2,8-DHA, mCPPD or MSU, 1 mg/mL, diluted in PBS) were injected directly into the air pouch. Six hours after crystal stimulation, air pouch lavages were performed and collected for cytokine quantification and cell isolation. Infiltrated cells were counted and phenotyped by flow cytometry. IL-1β cytokine production in supernatants or air pouch lavages was measured in the 6 animals (one missing data in the MSU group) by using ELISA kit (Invitrogen-Thermo fisher scientific, Waltham, MA, USA).

2.3.2. *Flow cytometry*

10^5 cells from air pouch lavages were stained with anti-F4/80-APC (clone REA126; Miltenyi Biotechnology, Bergish Gladbach, Germany) and anti-Ly6G-PE mouse monoclonal antibodies and clone 1A8 (Miltenyi Biotechnology, Bergish Gladbach, Germany) for 20 min at 4 °C, washed in PBS and analyzed with a BD FACS Canto II cytometer (BD Biosciences, Franklin Lakes, NJ, USA). Data were analyzed with BDFACS Diva software (BD Biosciences, Franklin Lakes, NJ, USA).

2.3.3. *Adenine model*

Thirty-two animals had a free access to tap water and received adenine enriched diet (chow containing 0.25% adenine, A8626 Sigma Aldrich, St-Louis, MO, USA) during 4 weeks to induce a 2,8-DHA nephropathy. After two weeks of adenine-enriched diet, animals were divided in 4 groups of 8 animals: control, allopurinol, dexamethasone and allopurinol, anakinra and allopurinol. Except control animals, all groups received allopurinol in tap water at 250 mg/L during the 2 last weeks as the standard therapy against 2,8-DHA. Each group received 100 µL/day subcutaneous injections during these two last weeks, with either isotonic sodium chloride (control and allopurinol groups), dexamethasone (1 mg/kg/day–Mylan, Canonsburg, PA, USA) or anakinra (100 mg/kg/day–Sobi France, Puteaux, France).

Animals were sacrificed 4 weeks after initiation of the adenine-enriched diet, blood and kidneys were collected. Blood samples were collected to assess serum urea, serum creatinine and serum uric acid levels with an IDS-iSYS automat (Immunodiagnostic Systems Holdings PLC, Pouilly-en-Auxois, France).

Left kidneys were fixed in formaldehyde and embedded in paraffin. X-ray computed tomography imaging of the left kidney was performed using a Skyscan 1272 (Bruker, Anvers, Belgium). A 6 µm resolution scale was obtained. Data were reconstructed using N-recon software (Bruker, Anvers, Belgium). The Mimics Innovation suite 20.0 (Materialise, Leuven, Belgium) was used to perform three-dimensional modeling of crystalline deposits in the kidney and quantify crystalline volume. Four-µm thick sections were stained with Masson trichromic solution and Hematoxylin/Eosin standard protocol

to reveal 2,8-DHA deposits in polarized light, or with sirius red in picric acid solution to assess fibrosis. A morphometric analysis of fibrosis tissue surface was performed with the Image J software (NIH) on 5 representative fields at ×200 magnification by using polarized light. For each animal, the mean value has been considered.

Crystalline deposits observed in tissue sections were characterized using FTIR microscopy as described above. Four-µm tissue sections were deposited on low-emission microscope slides (MirrIR; Keveley Technologies, Tienta Sciences, Indianapolis, USA) and FTIR hyperspectral images were recorded with a Spectrum spotlight 400 FT-IR imaging system (PerkinElmer, Waltham, USA).

2.3.4. *Quantitative RT-PCR*

mRNA from kidney was extracted using Trizol solution (Life Technologies BRL, Gaithersburg, MD, USA). RNA concentration was measured by using NanoDrop1000 spectrophotometer (Thermo Scientific, Waltham, MA, USA). RT-PCR was performed using SYBR green and specific probes on the light cycler 480 (Roche Diagnostic). Specific primers for TNF-α ForTCTTCTCATTCCTGCTTGTGG, RevATGAGAGGGAGGCCATTTG and IL1-β ForTGTAATGAAAGACGGCACACC RevTCTTCTTTGGGTATTGCTTGG, PCR was also carried out for the housekeeping gene HPRT ForGGAGCGGTAGCACCTCCT RevCTGGTTCATCATCGCTAATCAC to normalize the Q-PCR results, using Roche LightCycler 2.0 software (Roche Diagnostics Indianapolis, IN, USA). Results are expressed as $2^{-\Delta\Delta CT}$, where CT is the cycle threshold number.

2.4. *Statistical analyses*

Data are expressed as mean (±SEM). Data were analyzed with non-parametric tests (Kruskal Wallis followed by post hoc tests and Mann–Whitney test), using Statview and GraphPad Prism 7.0 softwares (GraphPad Software Inc., San Diego, CA, USA). The level of significance was set at <0.05.

3. Results

3.1. *Clinical study*

The histological lesions and the presence and type of inflammatory cells were assessed in kidney biopsies

from 17 patients, including 12 biopsies performed in renal transplant recipients. Acute tubular lesions were noticed in all biopsies and features of tubular atrophy and interstitial fibrosis were significant in 14 biopsies. Crystallites morphology was heterogeneous with irregular structures ($N = 17$), round shaped ($N = 16$) or ring-shaped ($N = 10$) deposits (Figure 1A–D). Crystallites were present in the tubular lumen ($N = 16$), in tubular cells ($N = 17$) and in the interstitial tissue ($N = 12$). Under polarized light, deposits were frequently radial ($N = 17$), sometimes needle-like ($N = 7$) and the typical "maltese cross" aspect was evidenced in 6 biopsies. In all biopsies, the presence of 2,8-DHA had been previously confirmed by FTIR microscopy. Scanning electron microscopy revealed the topography of the birefringent deposits (Figure 1E).

The presence of epithelioid granuloma was observed in 15/17 biopsies (88%). These granulomas were centered by 2,8-DHA crystals and made of epithelioid cells and giant multinucleated cells (Figure 1A–D). Immunostaining confirmed that granulomas contained mainly macrophages, with a predominance of macrophages type M2 (CD163+) over macrophages type M1 (CD68+), and T-cells (CD3+) (Figure 1F–H).

4. *In vivo* air-pouch model

To confirm whether 2,8-DHA crystals may induce an innate immune response, an air-pouch model was generated in C57Bl/6J mice. In this model, MSU crystals and monoclinic pyrophosphate dihydrate (mCPPD) crystals were used as a positive control to induce white blood cell chemotaxis, and IL-1β synthesis. 2,8-DHA crystals increased significantly white blood cell recruitment at 6 h in the air-pouch in comparison with controls ($p = 0.002$, $n = 6$/group, Figure 2A) but also in comparison with MSU ($p = 0.01$, $n = 6$/group). The number of macrophages was significantly increased by 2,8-DHA crystals in comparison with control and MSU crystals ($p = 0.002$ and $p = 0.01$ respectively, $n = 6$/group, Figure 2B), as well as the number of neutrophils ($p = 0.002$ vs controls and MSU crystals, $n = 6$/group, Figure 2C). IL-1β synthesis was also significantly increased by 2,8-DHA crystals in comparison with controls ($p = 0.01$, $n = 6$/group, Figure 2D), but there was a non-significant trend toward higher IL-1β in animals exposed to mCPPD and MSU crystals in comparison with controls.

5. *In vivo* 2,8-DHA nephropathy model

Exposure of mice to a diet enriched in adenine led to the precipitation of crystals in kidney tubules, and FTIR spectroscopic microscopy performed in several control mice confirmed that crystals were actually made of 2,8-DHA (Figure 3A,B). To assess the amount of crystallites in the kidneys, a 3-dimensional assessment of the whole-kidney crystalline volume was measured by CT-scan and evidenced that allopurinol, alone or in association with dexamethasone or anakinra, reduced significantly the volume of 2,8-DHA deposits as expected when compared to control group ($p = 0.0002$, $p = 0.0002$ and $p = 0.0003$ respectively, $N = 8$/group, Figure 4F). The addition of corticosteroids or anakinra to allopurinol did not reduce further the whole crystalline volume in comparison with allopurinol alone ($p = NS$, $n = 8$/group, Figure 4F).

Renal function was impaired in all groups of mice exposed to 2,8-DHA. Serum creatinine level was significantly higher in control mice than in groups receiving allopurinol alone ($p = 0.019$, $N = 8$/group Figure 5A), allopurinol+dexamethasone or allopurinol+anakinra ($p = 0.02$ and $p = 0.01$, respectively, $n = 8$/group, Figure 5A). Of note, mice exposed to anakinra and allopurinol had a lower serum creatinine level than mice exposed to allopurinol alone ($p = 0.009$, $N = 8$/group, Figure 5A). Serum urea level was lower in the anakinra+allopurinol group when compared to the control group ($p = 0.037$, $n = 8$/group, Figure 5B) but also in comparison with allopurinol and allopurinol+dexamethasone groups ($p = 0.02$ and 0.028, respectively, $N = 8$/group, Figure 5B). Renal fibrosis assessed by morphometry (sirius red in polarized light) was also significantly decreased in mice treated with anakinra and allopurinol when compared to controls ($p = 0.01$, $N = 8$/group (Figure 5C,D). A non-significant trend toward less fibrosis was observed in mice receiving allopurinol and allopurinol+dexamethasone. Unexpectedly, the expression of IL-1β was markedly increased in mice treated with allopurinol alone when compared to controls ($p = 0.028$, $N = 8$/group, Figure 5E), despite a lower number of crystalline deposits. Mice exposed to anakinra/allopurinol had a
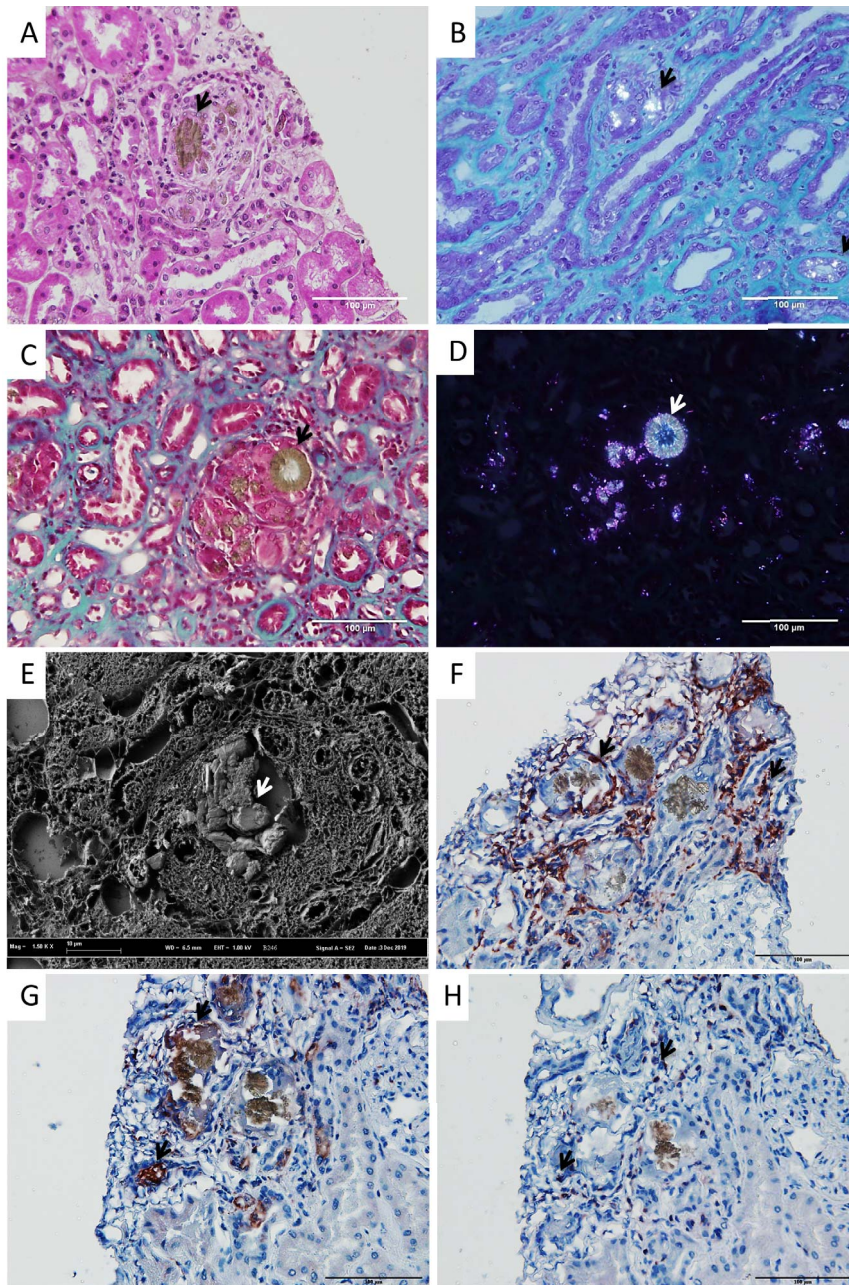
Figure 1. Typical crystalline deposits in kidney biopsies from patients affected by 2,8-DHA nephropathy. Crystallites were present in the tubular lumen and in the interstitial tissue and were frequently surrounded by granuloma containing epithelioid and giant cells (arrows, Figure 1A–D). Polarized light evidenced the presence of crystals in interstitial tissue and tubular cells (Figure 1B) and inside granuloma (Figure 1D). Scanning electron microscopy revealed the topography of deposits (Figure 1E). Immunohistochemistry revealed the presence of M2 type macrophages (arrows, CD163+, Figure 1F: crop showing the organization of macrophages around crystals), M1 type macrophages (arrows, CD68+, Figure 1G: crop showing the organization of macrophages around crystals) and lymphocytes (arrows, CD3+, Figure 1H) in granulomas surrounding 2,8-DHA crystallites. Negative controls did not evidence significant background staining (not shown).
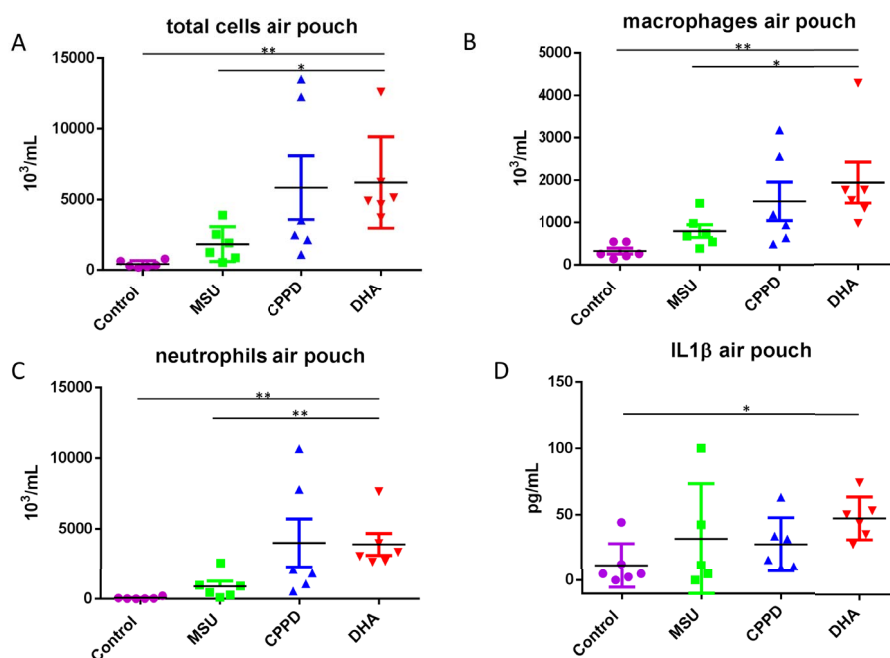
Figure 2. Air-pouch model. 2,8-DHA crystals increased significantly white blood cell recruitment at 6 h in the air-pouch in comparison with controls ([**] $p = 0.002$, $n = 6$/group, Figure 2A) but also in comparison with MSU ([*] $p = 0.01$, $n = 6$/group, Figure 2A). The number of macrophages was significantly increased by 2,8-DHA crystals in comparison with control and MSU crystals ([**] $p = 0.002$ and [*] $p = 0.01$ respectively, $n = 6$/group, Figure 2B), as well as the number of neutrophils ([**] $p = 0.002$ vs controls and MSU crystals, $n = 6$/group, Figure 2C). There was no significant difference in white blood cells recruitment between mCPPD and DHA crystals (Figure 2A–C). IL-1β synthesis was also significantly increased by 2,8-DHA crystals in comparison with controls ([*] $p = 0.01$, $n = 5$ or 6/group, Figure 2D). MSU: Monosodium urate; mCPPD: monoclinic calcium pyrophosphate dihydrate.

lower expression of IL-1β than controls and mice exposed to allopurinol alone ($p = 0.015$ and 0.0002, respectively, $N = 8$/group, Figure 5E). Mice exposed to allopurinol+dexamethasone had a lower expression of IL-1β than mice exposed to allopurinol alone ($p = 0.015$, $N = 8$/group, Figure 5E). TNF-α was reduced only in the allopurinol+anakinra group vs allopurinol alone ($p = 0.01$, $N = 8$/group, Figure 5F). Inflammatory infiltrate was less important in mice treated with anakinra and corticosteroids but infiltrates and granuloma were focal and therefore difficult to quantify (Figure 6).

6. Discussion

We describe herein that granuloma are frequent in a large series of kidney biopsies from patients affected

by 2,8-DHA nephropathy and that 2,8-DHA crystals induce an important innate immune response *in vivo*. Moreover, in a murine model of 2,8-DHA nephropathy, anakinra and dexamethasone, combined with allopurinol, improved renal function to a larger extent than allopurinol alone, the current standard therapy.

The lesions observed in kidney biopsies from patients affected by APRT deficiency have been described since decades but little attention has been paid to granuloma and inflammatory infiltrates. By contrast, inflammation and the role of the NLRP3 inflammasome have been described more extensively in 2,8-DHA murine models, promoted by adenine-enriched diet [21,22]. It has been evidenced that NLRP3 pharmacological inhibition, limiting innate immunity and inflammation, could be protective
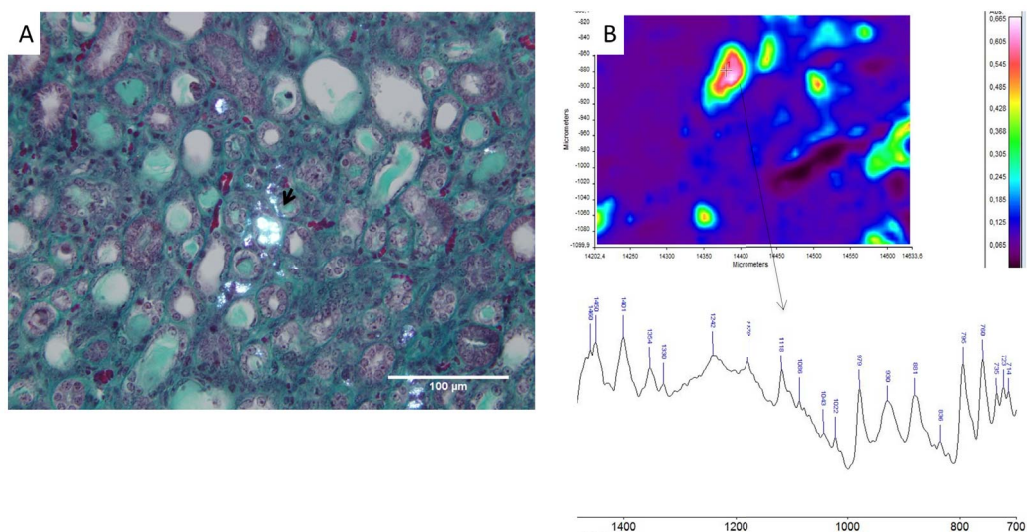
Figure 3. 2,8-DHA murine model. Typical crystals observed in polarized light after 4 weeks of adenine-enriched diet in kidney tissue in a control mouse (Figure 3A). FTIR microscopic analysis confirmed the nature of the crystalline phase: 2,8-DHA (Figure 3B, representative spectrum).

against crystalline nephropathies induced by calcium oxalate or 2,8-DHA crystal deposits [21,23, 24]. More recently, the presence of granuloma in a murine model of 2,8-DHA nephropathy has been highlighted [19].

As we observed massive inflammatory infiltrates and large granuloma in a series of human biopsies, we hypothesized that targeting innate immune pathways could be protective against renal lesions induced by 2,8-DHA, in addition to the conventional therapy (allopurinol or febuxostat). Actually, among 17 biopsies with FTIR-proven 2,8-DHA crystals in the tissue, epithelioid granuloma were present in 15 biopsies and centered by 2,8-DHA crystallites. 2,8-DHA crystals induced IL-1β synthesis *in vivo*, a result consistent with the biological effect of other particulate inflammasome activators, particularly sodium urate [25]. Interestingly, it has been shown recently in a rodent model of 2,8-DHA nephropathy that TNF receptor 1 was an important mediator of crystal clearance and inflammation [19]. Mice deficient in *Tnfr* 1 gene have reduced lesions and inflammation when exposed to 2,8-DHA nephropathy. In the view of these results the authors suggested that targeting the TNF/TNFR pathway could be a potential option to treat 2,8-DHA nephropathy, as previously shown in calcium oxalate nephropa-

thy [26]. Although TNF-α is a potentially interesting target, we focused our attention on IL-1β because drugs inhibiting IL-1β pathway have been shown to be efficient in crystallopathies, especially gout and chondrocalcinosis [27]. In the air pouch model, the dramatic increase in IL-1β synthesis in response to 2,8-DHA crystals which correlated with white blood cell recruitment, led us to test drugs interfering with innate immunity in a murine 2,8-DHA model, dexamethasone and anakinra. The two murine models were complementary: the air-pouch model allowed a precise quantification of white-blood cells recruitment and IL-1β synthesis in response to 2,8-DHA crystals, whereas the 2,8-DHA nephropathy model highlighted the role of anti-inflammatory drugs, in addition to allopurinol, on renal function and renal tissue lesions. To date, the gold standard therapy against 2,8-DHA nephropathy is xanthine oxidoreductase inhibition, by allopurinol and in some cases febuxostat [17]. These drugs inhibit the conversion of adenine, produced in excess due to APRT deficiency, to 2,8-DHA which precipitates in urine. This lifelong therapy can prevent urolithiasis recurrence, stabilize renal function and sometimes ameliorate the glomerular filtration rate if prescribed early, but renal function recovery may be incomplete, especially after acute renal failure episodes [6,7]. In the
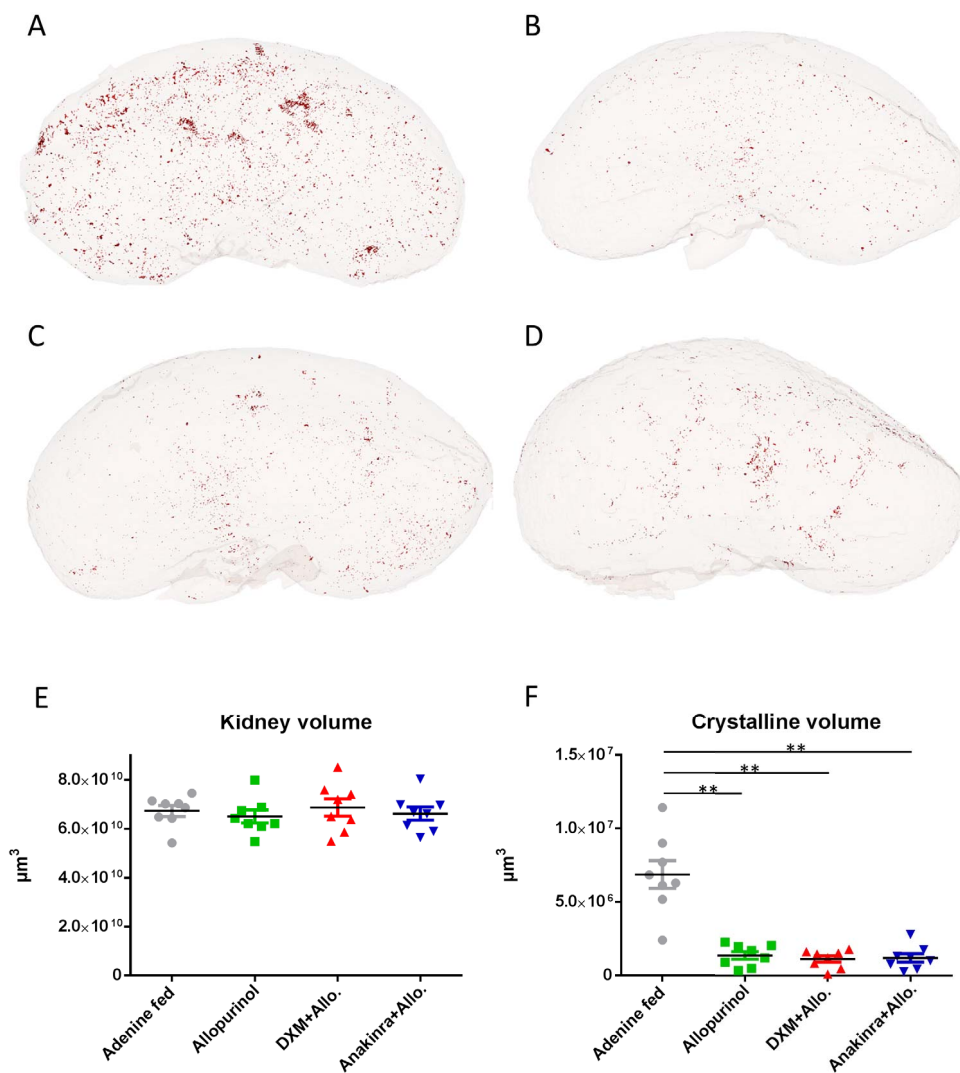
Figure 4. 3D measurement of crystalline volume. The 3-dimensional assessment of the crystalline volume was measured by CT-scan in the adenine fed (control) group (Figure 4A, 2,8-DHA crystallites in red), allopurinol group (Figure 4B), allopurinol+dexamethasone (Figure 4C) and allopurinol+anakinra (Figure 4D). Total volume of the kidneys was not affected by treatment in any group (Figure 4E). Allopurinol reduced significantly the volume of 2,8-DHA deposits as expected when compared to control group (** $p = 0.0002$, Figure 4F). Crystalline volume reduction was also significant (vs adenine fed controls) in the allopurinol+dexamethasone (DXM+Allo.) and in the allopurinol+anakinra (Anakinra+Allo.) groups (** $p = 0.0002$ and $p = 0.0003$ respectively, $N = 8$/group, Figure 4F). The addition of dexamethasone or anakinra to allopurinol did not reduce further the whole crystalline volume in comparison with allopurinol alone ($p = $ NS, $n = 8$/group, Figure 4F). DXM: dexamethasone; Allo.: allopurinol.

view of human renal histology and air-pouch model results, we hypothesized that anti-inflammatory drugs could be of help in a murine model of 2,8-DHA, in addition to allopurinol, the standard therapy. Although non-specific, corticosteroids are still the main drugs used to control innate immunity, and have been shown to be efficient in renal granulomatous diseases such as sarcoidosis [28]. Anakinra
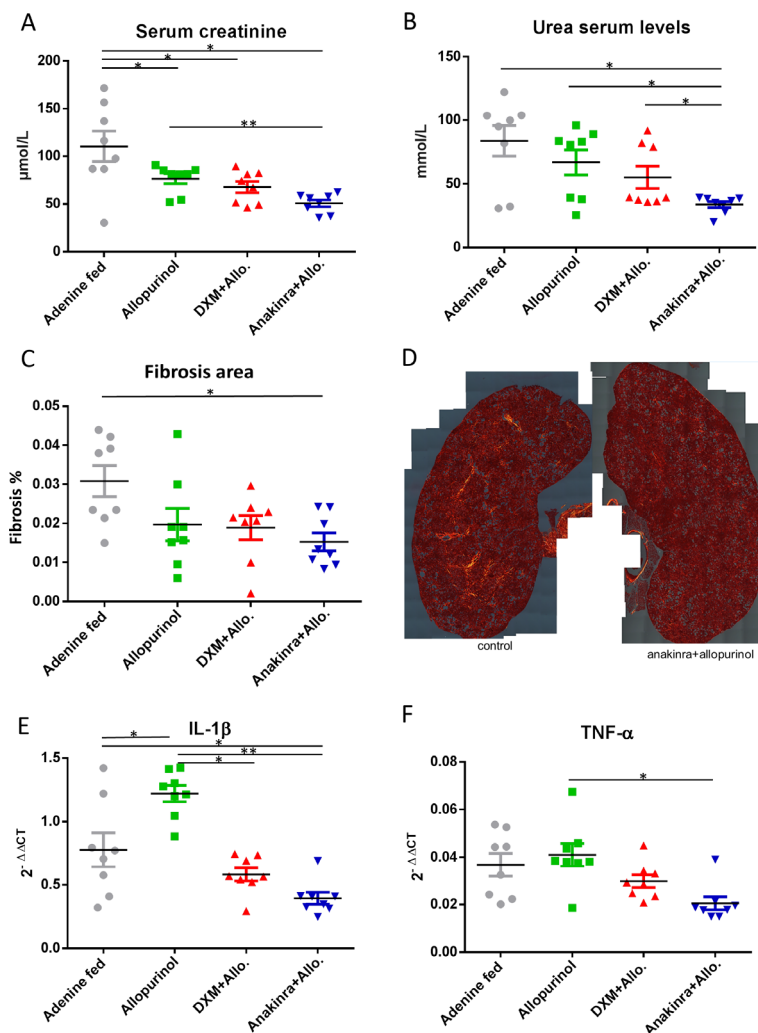
Figure 5. Renal function, inflammation and fibrosis. Serum creatinine was significantly higher in control adenine fed mice than in groups receiving allopurinol alone ($^*p$ = 0.019, N = 8/group Figure 5A), allopurinol+dexamethasone (DXM+Allo.) or allopurinol+anakinra (Anakinra+Allo.) ($^*p$ = 0.02 and $^*p$ = 0.01, respectively, n = 8/group, Figure 5A). Mice exposed to anakinra and allopurinol had a lower serum creatinine level than mice exposed to allopurinol alone ($^{**}p$ = 0.009, N = 8/group, Figure 5A). Serum urea levels were improved in the allopurinol+anakinra group when compared to control group ($^*p$ = 0.037, n = 8/group, Figure 5B) but also in comparison with allopurinol and allopurinol+dexamethasone groups ($^*p$ = 0.02 and 0.028, respectively, N = 8/group, Figure 5B). Renal fibrosis assessed by morphometry (sirius red in polarized light) was significantly decreased in mice treated with allopurinol+anakinra when compared to controls ($^*p$ = 0.01, N = 8/group, Figure 5C,D; mosaics: left: control kidney, right: allopurinol+anakinra kidney). A non-significant trend toward less fibrosis was observed in mice receiving allopurinol and allopurinol/steroids. The expression of IL-1β was markedly increased in mice treated with allopurinol alone when compared to controls ($^*p$ = 0.028, N = 8/group, Figure 5E). Mice exposed to allopurinol+anakinra had a lower expression of IL-1β than controls and mice exposed to allopurinol alone ($^*p$ = 0.015 and **0.0002, respectively, N = 8/group, Figure 5E). Mice exposed to allopurinol+dexamethasone had a lower expression of IL-1β than mice exposed to allopurinol alone ($^*p$ = 0.015, N = 8/group, Figure 5E). TNF-α was reduced only in the anakinra/allopurinol group vs allopurinol alone ($^*p$ = 0.01, N = 8/group, Figure 5F). IL-1β: interleukin-1 beta; TNF-α: Tumor necrosis factor alpha; DXM: dexamethasone; Allo.: allopurinol.
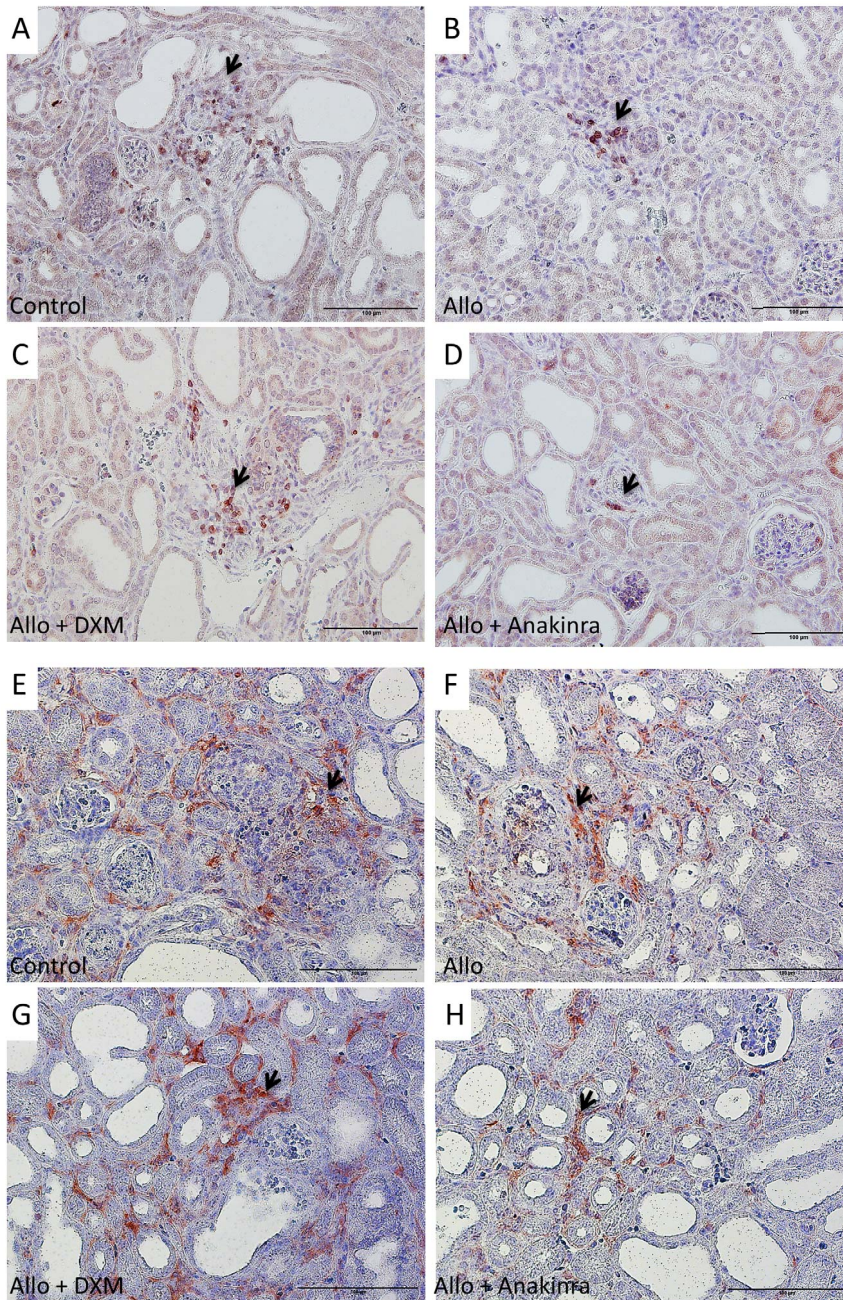
Figure 6. Inflammatory infiltrate in the murine model of nephropathy. Lymphocytes infiltrate (anti CD3 antibody) was less important in mice treated with anakinra (Figure 6D) and to a lesser extent with DXM (Figure 6C) than in control mice (Figure 6A) and in mice treated with allopurinol alone (Figure 6B). Macrophages (anti pan-macrophages antibody) were less present in mice treated with anakinra (Figures 6H) and DXM (Figure 6G) than in control mice (Figure 6E) and in mice treated with allopurinol alone (Figure 6F). Negative controls evidenced a mild background staining (not shown). DXM: dexamethasone; Allo: allopurinol.

is a recombinant, and slightly modified, human interleukin 1 receptor antagonist protein. It has been developed to treat rheumatoid arthritis and is also useful to manage gout attacks and to a larger extent diseases involving NLRP3 inflammasome activation and IL-1β synthesis [27].

The addition of anakinra or dexamethasone to allopurinol improved significantly renal function and renal lesions in the murine model of 2,8-DHA nephropathy. Of note, dexamethasone may have increased serum urea levels through its catabolic effect, limiting the decrease in serum urea due to improvement of renal function. Interestingly, allopurinol decreased significantly, as expected, the amount of crystalline deposits in renal tissue but the addition of steroids or anakinra did not reduce further the crystalline global volume, suggesting that these anti-inflammatory drugs protected renal tissue against fateful damages induced by inflammation and fibrosis but did not reduce significantly crystal adhesion or retention in tubules.

Anakinra has already been tested in another crystalline nephropathy model induced by calcium-oxalate tubular crystallites. Mulay *et al.* have shown first that IL-1 blockade by anakinra protected from renal failure in calcium oxalate nephropathy but in more recent models, anakinra did not improve renal function in a calcium oxalate nephropathy model [23,24]. In a murine model of 2,8-DHA crystalline nephropathy, inhibition of NLRP3 inflammasome by a specific inhibitor had demonstrated its efficiency to reduce IL-1β synthesis and kidney fibrosis [21]. One may hypothesize that purine-mediated IL-1β synthesis may be particularly important in response to 2,8-DHA crystals.

The most surprising observation was the significantly increased expression of IL-1β and TNF-α in the kidneys of mice treated with allopurinol alone. It seems unlikely that allopurinol by itself would be pro-inflammatory and we have no clear explanation but a parallel may be drawn with another crystallopathy: gout. Actually, the onset of treatments decreasing serum urate levels in gouty patients is associated with acute gout flares. The underlying mechanism is unknown but it has been hypothesized that urate lowering may lead to large crystals or tophi destabilization and induce pro-inflammatory pathways, this is the reason why allopurinol and febuxostat are classically associated with colchicine to prevent gout flares during the first months of the therapy [29]. One may also hypothesize that in the 2,8-DHA nephropathy model, allopurinol would be overall beneficial by lowering 2,8-DHA crystals formation (as observed in our model) but, on the other hand, could "activate" transiently pro-inflammatory pathways through destabilization of 2,8-DHA crystallites. This mechanism remains hypothetical to date and deserves further studies but this observation stresses even more the potential benefit of a short-term therapy based upon steroids or anakinra when initiating the treatment of 2,8-DHA nephropathy by allopurinol or febuxostat.

One of the main strength of our study is the demonstration, in a significant number of human biopsies and in murine models, that inflammation plays a role in the lesions induced by 2,8-DHA crystals. The significant improvement of renal function by anakinra and dexamethasone definitively proves the key role of innate immunity in this model and opens new potential clinical perspectives. Our study has some limitations. In murine *in vivo* models, we evidenced that cytokine synthesis was decreased significantly in mice exposed to anakinra and dexamethasone but, unlike in the air pouch model, we could not quantify precisely the number of immune cells in the kidney tissue. Moreover, although we confirmed that the crystalline deposits were actually made of 2,8-DHA, the *in vivo* model is based upon administration of adenine, and not a genetic murine model based upon APRT deficiency [30,31].

As a conclusion, inflammation and innate immunity play a critical role in 2,8-DHA nephropathy. Steroids or drug targeting IL-1 pathway are efficient to protect renal function and tissue in experimental models, when added to the standard therapy. As the disease is rare, it does not seem feasible to test these drugs in a randomized controlled study but the risk of a transient treatment by steroids or anakinra seems low in comparison with the potential benefit. The observation of granuloma in the renal biopsy could be of help before initiating this type of treatment. For instance, there is no doubt that steroids are useful against granulomatous lesions due to renal sarcoidosis. Unfortunately, APRT deficiency is frequently diagnosed in renal transplant recipients: the use of corticosteroids has decreased in renal transplantation during the past decades, in the view of their long-term side effects, but a transient treatment targeting

innate immunity when inflammatory infiltrate is observed in the graft seems a reasonable option, especially when allopurinol or febuxostat is initiated. Additional studies are still warranted, including the assessment of plasma and/or urinary biomarkers for inflammatory activity in the kidney of patients affected by 2,8-DHA nephropathy.

References

[1] G. Bollée, J. Harambat, A. Bensman, B. Knebelmann, M. Daudon, I. Ceballos-Picot, *Clin. J. Am. Soc. Nephrol.*, 2012, **7**, 1521-1527.

[2] I. Ceballos-Picot, J. L. Perignon, M. Hamet, M. Daudon, P. Kamoun, *Lancet*, 1992, **339**, 1050-1051.

[3] Y. Hidaka, T. D. Palella, T. E. O'Toole, S. A. Tarlé, W. N. Kelley, *J. Clin. Investig.*, 1987, **80**, 1409-1415.

[4] V. Edvardsson, R. Palsson, I. Olafsson, G. Hjaltadottir, T. Laxdal, *Am. J. Kidney Dis.*, 2001, **38**, 473-480.

[5] E. R. Gagné, E. Deland, M. Daudon, L. H. Noël, T. Nawar, *Am. J. Kidney Dis.*, 1994, **24**, 104-107.

[6] G. Bollée, P. Cochat, M. Daudon, *Can. J. Kidney Health Dis.*, 2015, **2**, article no. 31.

[7] M. Zaidan, R. Palsson, E. Merieau, E. Cornec-Le Gall, A. Garstka, U. Maggiore, P. Deteix, M. Battista, E.-R. Gagné, I. Ceballos-Picot, J.-P. Duong Van Huyen, C. Legendre, M. Daudon, V. O. Edvardsson, B. Knebelmann, *Am. J. Transplant.*, 2014, **14**, 2623-2632.

[8] I. Ceballos-Picot, M. Daudon, J. Harambat, A. Bensman, B. Knebelmann, G. Bollée, *Nucleosides Nucleotides Nucleic Acids*, 2014, **33**, 241-252.

[9] G. Bollée, C. Dollinger, L. Boutaud, D. Guillemot, A. Bensman, J. Harambat, P. Deteix, M. Daudon, B. Knebelmann, I. Ceballos-Picot, *J. Am. Soc. Nephrol.*, 2010, **21**, 679-688.

[10] A. Sahota, J. Chen, S. A. Boyadjiev, M. H. Gault, J. A. Tischfield, *Hum. Mol. Genet.*, 1994, **3**, 817-818.

[11] N. Kamatani, M. Hakoda, S. Otsuka, H. Yoshikawa, S. Kashiwazaki, *J. Clin. Investig.*, 1992, **90**, 130-135.

[12] V. O. Edvardsson, D. S. Goldfarb, J. C. Lieske, L. Beara-Lasic, F. Anglani, D. S. Milliner, R. Palsson, *Pediatr. Nephrol.*, 2013, **28**, 1923-1942.

[13] H. L. Runolfsdottir, J. A. Sayer, O. S. Indridason, V. O. Edvardsson, B. O. Jensson, G. A. Arnadottir, S. A. Gudjonsson, R. Fridriksdottir, H. Katrinardottir, D. Gudbjartsson, U. Thorsteinsdottir, P. Sulem, K. Stefansson, R. Palsson, *Eur. J. Hum. Genet.*, 2021, 1061-1070.

[14] M. Daudon, P. Jungers, *Nephron Physiol.*, 2004, **98**, 31-36.

[15] V. Frochot, M. Daudon, *Int. J. Surg.*, 2016, **36**, 624-632.

[16] G. Garigali, G. Marra, V. Rizzo, F. de Liso, A. Berrettini, M. Daudon, G. B. Fogazzi, *Clin. Chim. Acta*, 2019, **492**, 23-25.

[17] V. O. Edvardsson, H. L. Runolfsdottir, U. A. Thorsteinsdottir, I. M. S. Agustsdottir, G. S. Oddsdottir, F. Eiriksson, D. S. Goldfarb, M. Thorsteinsdottir, R. Palsson, *Eur. J. Intern. Med.*, 2018, **48**, 75-79.

[18] H. L. Runolfsdottir, R. Palsson, I. M. S. Agustsdottir, O. S. Indridason, J. Li, M. Dao, B. Knebelmann, D. S. Milliner, V. O. Edvardsson, *Transplantation*, 2020, **104**, 2120-2128.

[19] B. M. Klinkhammer, S. Djudjaj, U. Kunter, R. Palsson, V. O. Edvardsson, T. Wiech, M. Thorsteinsdottir, S. Hardarson, O. Foresto-Neto, S. R. Mulay, M. J. Moeller, W. Jahnen-Dechent, J. Floege, H.-J. Anders, P. Boor, *J. Am. Soc. Nephrol.*, 2020, **31**, 799-816.

[20] P. Gras, C. Rey, O. Marsan, S. Sarda, C. Combes, *Eur. J. Inorg. Chem.*, 2013, **2013**, 5886-5895.

[21] I. Ludwig-Portugall, E. Bartok, E. Dhana, B. D. G. Evers, M. J. Primiano, J. P. Hall, B. S. Franklin, P. A. Knolle, V. Hornung, G. Hartmann, P. Boor, E. Latz, C. Kurts, *Kidney Int.*, 2016, **90**, 525-539.

[22] C. Okabe, R. L. Borges, D. C. de Almeida, C. Fanelli, G. P. Barlette, F. G. Machado, S. C. A. Arias, D. M. A. C. Malheiros, N. O. S. Camara, R. Zatz, C. K. Fujihara, *Am. J. Physiol. Renal. Physiol.*, 2013, **305**, F155-F163.

[23] H.-J. Anders, B. Suarez-Alvarez, M. Grigorescu, O. Foresto-Neto, S. Steiger, J. Desai, J. A. Marschner, M. Honarpisheh, C. Shi, J. Jordan, L. Müller, N. Burzlaff, T. Bäuerle, S. R. Mulay, *Kidney Int.*, 2018, **93**, 656-669.

[24] S. R. Mulay, O. P. Kulkarni, K. V. Rupanagudi, A. Migliorini, M. N. Darisipudi, A. Vilaysane, D. Muruve, Y. Shi, F. Munro, H. Liapis, H.-J. Anders, *J. Clin. Investig.*, 2013, **123**, 236-246.

[25] F. Martinon, V. Pétrilli, A. Mayor, A. Tardivel, J. Tschopp, *Nature*, 2006, **440**, 237-241.

[26] S. R. Mulay, J. N. Eberhard, J. Desai, J. A. Marschner, S. V. R. Kumar, M. Weidenbusch, M. Grigorescu, M. Lech, N. Eltrich, L. Müller, W. Hans, M. Hrabĕ de Angelis, V. Vielhauer, B. Hoppe, J. Asplin, N. Burzlaff, M. Herrmann, A. Evan, H.-J. Anders, *J. Am. Soc. Nephrol.*, 2017, **28**, 761-768.

[27] A. So, T. De Smedt, S. Revaz, J. Tschopp, *Arthritis Res. Ther.*, 2007, **9**, article no. R28.

[28] R. Bergner, C. Löffler, *Curr. Opin. Pulm. Med.*, 2018, **24**, 513-520.

[29] A. Latourte, T. Bardin, P. Richette, *Rheumatology (Oxford)*, 2014, **53**, 1920-1926.

[30] S. J. Engle, M. G. Stockelman, J. Chen, G. Boivin, M. N. Yum, P. M. Davies, M. Y. Ying, A. Sahota, H. A. Simmonds, P. J. Stambrook, J. A. Tischfield, *Proc. Natl. Acad. Sci. USA*, 1996, **93**, 5307-5312.

[31] N. J. Redhead, J. Selfridge, C. L. Wu, D. W. Melton, *Hum. Gene Ther.*, 1996, **7**, 1491-1502.